ELSEVIER

3 April 2000

Physics Letters A 268 (2000) 104–111

PHYSICS LETTERS A

www.elsevier.nl/locate/physleta

Enhanced backscattering from photonic crystals

A. Femius Koenderink *, Mischa Megens [1], Gijs van Soest, Willem L. Vos, Ad Lagendijk

Van der Waals-Zeeman Instituut, Universiteit van Amsterdam, Valckenierstraat 65, NL-1018 XE Amsterdam, The Netherlands

Received 16 February 2000; accepted 22 February 2000
Communicated by L.J. Sham

Abstract

We have studied enhanced backscattering of both polystyrene opals and strongly photonic crystals of air spheres in TiO_2 in the wavelength range of first and higher order stop bands. The shape of the enhanced backscattering cones is well described by diffusion theory. We find transport mean free paths of the order of 15 μm both for opals and air spheres. Close to the stop band the cone width is decreased due to internal reflections generated by the photonic band structure. Widening occurs due to attenuation of the coherent beam by Bragg scattering. We present a model that incorporates these effects and successfully explains the data. © 2000 Elsevier Science B.V. All rights reserved.

PACS: 42.70.Qs; 42.25.Dd; 42.25.Hz

1. Introduction

Currently there is much interest in creating ordered optical materials known as photonic crystals [1,2]. Periodic variations of the refractive index on lengths of the order of the wavelength of light result in stop bands for propagation in certain directions. If the light is very strongly coupled to the crystal a photonic band gap is expected, i.e. a frequency range for which there are no optical modes at all [1]. The interest in photonic band gaps is mainly driven by the prospect of novel phenomena in optics and quantum optics, such as inhibition of spontaneous emission [1,2]. The emphasis is on creating favorable three dimensional structures with a very high refractive index contrast. It turns out that the resulting crystals not only diffract the light strongly. Disorder, which is always present in the fabricated structures, gives rise to considerable random scattering. These effects can not be explained by theories [1,2] based on perfect photonic crystals. As John [3] first pointed out, disorder in photonic crystals is of fundamental interest for the observation of Anderson localization of light. Anderson localization [4,5] of light is a delicate interference effect in multiple scattering of light in disordered optical materials, such as GaAs powders [6] and the novel macroporous GaP structures [7].

Enhanced backscattering is an interference phenomenon by which the transport of light in a multi-

* Corresponding author.
E-mail address: fkoender@wins.uva.nl (A. Femius Koenderink).
[1] Present address: Department of Physics, Princeton University, Princeton, New Jersey 08544, USA.

PII: S0375-9601(00)00153-5

ple scattering medium can be studied [8–12]. The intensity scattered by an object exhibits a clear maximum in the exact backscatter direction, which results from constructive interference of counterpropagating light paths. It is well established that a triangular peak superimposed on the diffuse background results [8–12]. The width of this 'enhanced backscattering cone' is inversely proportional to the transport mean free path ℓ, which determines the length of the light paths. The interference effect doubles the diffuse intensity in the exact backscatter direction. For disordered media the shape of the cone is accurately described by diffusion theory [12]. No experimental or theoretical study of random scattering in periodically inhomogeneous dispersive media exists, apart from a theoretical study concerned with electron waves [13] and an experimental study of the effect of disorder on optical transmission of photonic crystals [14].

We have studied enhanced backscattering both from opal photonic crystals and strongly photonic crystals consisting of air spheres in titania [15,16]. The effect of enhanced backscattering is especially suited to quantify the random scattering in photonic crystals since it inherently averages over the full sample volume. Backscattering cones were recorded for wavelengths in the range of the lowest order stop bands, to probe the interaction of the randomness inherently present in the samples with the photonic band structure. A striking result is that the shape of the enhanced backscattering cones is well described by the diffusion theory for disordered media [12]. The photonic crystals appear to be weakly scattering, since the transport mean free paths we observe are large compared to the wavelengths used. We have developed a model based on diffusion theory which shows that the width of the backscatter cone is increased in the stop band due to attenuation of the coherent beam, and decreased at the blue edge of the stop band due to Bragg-enhanced internal reflection. The model is consistent with the data.

2. Experiment

We have studied opals consisting of polystyrene spheres (Duke Scientific, polydispersity $\sim 2\%$) of which opals were made by sedimentation in 0.3 mm thick, 3 mm wide flat glass capillaries (Vitro Dynamics). The opals composed of spheres of radii 120, 180, 213, 241, 262 and 326 nm were grown from a suspension in water using a centrifuge. Crystals consisting of spheres of radius 403, 426 and 439 nm slowly sedimented under gravity and formed large domains (~ 1 mm). After crystallization the suspending liquid was slowly evaporated from the capillaries to obtain polycrystalline opals of 74 volume percent, which are more than 10 mm in length. The refractive index contrast is 1.59. Small-angle X-ray diffraction confirms that such crystals have an *fcc* structure [17]. These crystals are stacked with (111) planes along the capillary faces.

We measured enhanced backscattering cones of the polystyrene opals with the off-centered rotation technique [18]. The technique provides a high angular resolution of approximately 0.7 mrad with an illumination area of 2.5 mm in diameter. Cones were recorded using three different lasers operating at wavelengths of 632 nm (HeNe), 685 nm, and 780 nm (laser diodes). The incident light was linearly polarized and detection was in the polarization-conserving channel. Speckle averaging was performed by continuously varying the tilt of the samples. The illuminated spot was on the tilt axis, while the tilt amplitude was smaller than 6°.

To investigate a more strongly photonic material we studied an *fcc* crystal of air spheres in titania (refractive index contrast ~ 2.5). The crystal was made by filling the voids of an opal of polystyrene spheres of 180 nm radius with a precursor of TiO_2 and subsequently removing the polystyrene by calcination [15]. The sample, which is glued to the tip of a needle, has a rectangular shape with an area of around 1 mm^2 and it is about 200 μm thick. Small angle X-ray diffraction showed that the lattice parameter is 360 ± 10 nm and that the periodic structure extends all the way throughout the sample. Indeed, the sample shows colorful reflections on both sides [15,16].

We measured backscattering from the air-sphere crystals using a setup allowing continuous tuning of the wavelength. As a light source we used a parametric oscillator pumped by the third harmonic of a diode pumped Nd:YAG laser (Coherent XPO). The wavelength of the parametric oscillator is fully tunable over the visible spectrum, and its short coher-

ence length facilitates speckle averaging. The beam from the oscillator was collimated to a divergence of ~ 1 mrad; the beam diameter was ~ 0.5 mm at the position of the air-sphere crystal. The beam was incident on a (111) plane of the sample via a beam splitter which is wedged to avert ghost reflections. The backscattered intensity was collected on a CCD camera positioned in the focal plane of a positive lens. The detection was in the polarization-conserving channel. The sample was slightly tilted to keep the specular reflection from reaching the detector. Speckle averaging was performed by spinning the sample, averaging over multiple camera exposures, and averaging concentric circles in the two dimensional images. This setup is optimal in the sense that the resolving power ~ 1 mrad is mainly determined by the size of the sample, and convenient since it allows fast data acquisition.

3. Results

Fig. 1(a) shows the backscattered intensity of a polystyrene opal composed of spheres of radius 326 nm measured at a wavelength of 780 nm. A triangular peak superimposed on the diffuse background, which is scaled to unity, is observed in the backscatter direction $\theta = 0$. The enhancement factors, defined as the ratio between the intensity scattered in the exact backward direction and the diffuse background, range between 1.45 and 1.85 for the backscatter cones of opals. In the polarization conserving detection channel single scattering is also detected. Since single scattering paths do not have time reversed counterparts, single scattering contributes to the diffuse background only. Consequently, the cones are expected to have enhancement factors less than 2.

From the full width at half maximum W, typically 10 mrad for the opals, we estimate that the transport mean free path ℓ is of the order of $15\,\mu$m. Clearly ℓ is large compared to the wavelength $\lambda \sim 0.7\,\mu$m. The transport mean free path is also much longer than the sphere radii $r \leq 0.5\,\mu$m and larger than 10 times the lattice parameter.

We have found that backscatter cones of different opals composed of spheres of identical radius are of the same width within 10%. To study the effect of the capillary walls we have also measured enhanced backscattering from an opal which we removed from its capillary. No difference with the cone resulting from a duplicate opal still in its capillary was found. Visual inspection of the opals shows that the surface of the crystals is covered by colorful Bragg reflecting domains of various sizes, typically $\ll 1$ mm for the centrifuged samples ($r \leq$ 326 nm), and ~ 1 mm for the remaining opals. We studied samples of which the surface was partly covered by small, and partly by large domains. No correlation between cone width and the size of the domains was found. Enhanced backscattering inherently averages over the whole sample volume, while the Bragg reflec-

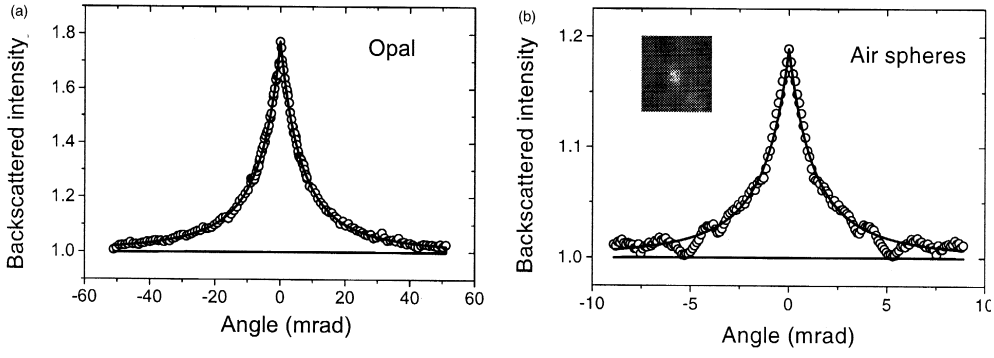

Fig. 1. The backscattered intensity normalized to the diffuse background as a function of angle θ for (a) an opal composed of spheres of radius 326 nm measured at a wavelength of 780 nm, and (b) the air-sphere crystal ($\lambda = 460$ nm). The curves are least-squares fits to the data of the cone shape predicted by diffusion theory for a disordered medium. For the air spheres we find the profile as a function of $|\theta|$ by integrating over circles concentric with the peak in the two-dimensional image (inset). The points $\theta < 0$ are duplicates of $\theta > 0$.

tions are determined by crystalline order close to the surface.

The backscatter cone of an air-sphere crystal ($\lambda = 460$ nm) is shown in Fig. 1(b). The inset shows the two dimensional image obtained from averaging multiple camera exposures. The backscatter cone shows as a bright spot. The backscattered intensity as a function of $|\theta|$ is obtained by averaging circles concentric with the intensity peak. To facilitate visual inspection the data is plotted both for $\theta > 0$ and $\theta < 0$. The enhancement factor observed in case of the air-sphere crystals is typically 1.3. We attribute the low enhancement factor to experimental limitations related to the small sample size. The width of the backscatter cones of the air-spheres is typically 5 mrad.

The solid lines in Figs. 1(a) and 1(b) are least-squares fits of the shape predicted by diffusion theory for the case of random, non-absorbing, semi-infinite slabs [12]. The only adjustable parameters are an overall scaling factor, the enhancement factor, and the width-determining parameter $\ell_W \approx 0.7 n_e (k_e W)^{-1}$ in terms of the full width at half maximum W of the cone. Here $k_e = (2\pi/\lambda) n_e$ is the wave vector of light in the medium of effective refractive index n_e. Diffusion theory describes the shape of the backscatter cones from our photonic crystals well, although the intensity scattered by the opal with $r = 120$ nm decreases more rapidly at large angles. It is remarkable that a theory developed to describe multiple scattering in random media fits the shape of backscatter cones originating from photonic crystals.

For random media without diffuse internal reflection ℓ_W is identical to the transport mean free path ℓ. For disordered media with an effective refractive index mismatch with the surroundings the cone is narrowed as a result of internal reflections [19]. As we discuss below, the value of ℓ_W may also be affected by the stop bands. It is instructive to consider the fitted length scale ℓ_W as a function of the size parameter $x = k_0 r = (2\pi/\lambda) r$ of the polystyrene spheres (Fig. 2(a)), or air spheres (Fig. 2(b)): both the scattering properties of the spheres and air holes, and the stop band frequencies of the crystals scale with x [20]. The frequencies of the (111) Bragg reflections in the relevant size parameter range were measured in a normal-incidence reflectivity measurement as described in Ref. [16]. We have indicated the red and blue edges of the associated L-gaps by vertical lines in Figs. 2(a) and 2(b). For the opals higher order stop bands are indicated by vertical marks.

For the opals the data are grouped by sample in Fig. 2(a) since comparison between different samples is a priori difficult due to possible differences in defect structure. The reproducibility of the cone width among sets of opals of identical spheres and the

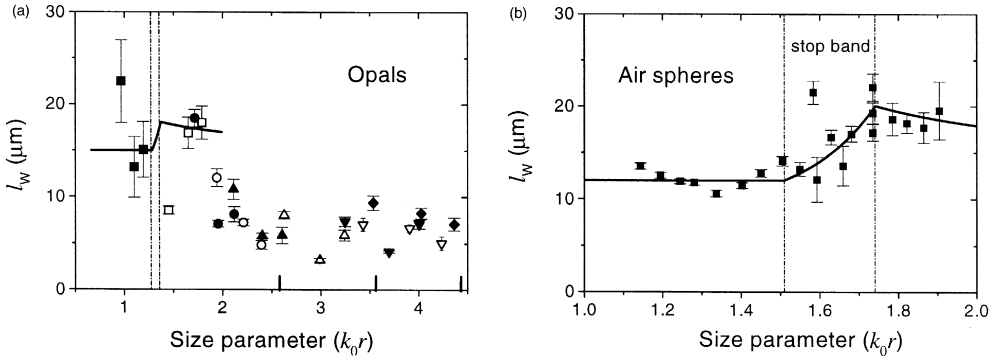

Fig. 2. (a) The width determining parameter ℓ_W as a function of the size parameter $x = (2\pi/\lambda) r$ for (a) all polystyrene samples (sphere radii 120 (■), 180 (□), 213 (●), 241 (○), 262 (▲), 326 (△), 403 (▼), 426 (▽), 439 nm (◆)) and (b) the air-sphere crystal. The red and blue edge of the first order L-gap are indicated in (a) and (b) by dashed vertical lines. In (a) higher order L-gap stop bands are indicated by vertical marks. The center frequencies of the stop bands are inferred from reflectivity spectra. The solid curves result from the diffusion model incorporating photonic crystal effects, and are scaled to match the value of ℓ_W at the red edge of the stop band. Apart from the scaling factor there is no adjustable parameter.

modest scatter suggest that a comparison over the whole size parameter range is allowed. A marked decrease of ℓ_W from 20 to 7 μm starting at the red side of the first order (111) stop band is observed followed by an increase at the blue edge. After a maximum near $x = 1.7$ the value of ℓ_W remains close to 7 μm.

The data from the air-sphere crystal (Fig. 2(b)) were acquired as a function of wavelength over the whole visible spectrum. An increase of ℓ_W from $\ell_W \approx 14\,\mu m$ starting at the red edge of the (111) stop band to $\ell_W \approx 20\,\mu m$ at the blue edge is observed for the air-sphere crystal.

4. Diffusion model incorporating photonic crystal effects

We expect the variation of ℓ_W close to the stop band to be caused by the photonic band structure. A Mie calculation [20] indeed shows that the scattering properties of the individual spheres in the opals and air-sphere crystal are nearly constant in the size parameter range of the stop band. The width of the cone is crucially influenced by the fact that the (111) planes are parallel to the sample surface, resulting in L-gaps which coincide with the incident and backscatter direction. Starting from the diffusion approach [12,19], we observe that the cone is affected by two different mechanisms, the first of which concerns the diffuse intensity, and the second the coherent beam.

The first mechanism applies to the diffuse intensity. Light paths returning to the sample surface at directions close to normal incidence suffer from internal reflection due to Bragg scattering (see Fig. 3). Internal reflection creates longer light paths, hence the cone becomes narrower [19].

The second effect results from the attenuation of the coherent beam due to Bragg scattering for frequencies in the L-gap. The cone is affected because the coherent beam acts as a source for the diffuse intensity. Due to the strong attenuation of the coherent beam at wavelengths within the stopband, the backscatter cone is predominantly composed of light paths starting very close to the sample surface. Since these light paths are shorter on average [12], this effect broadens the cone.

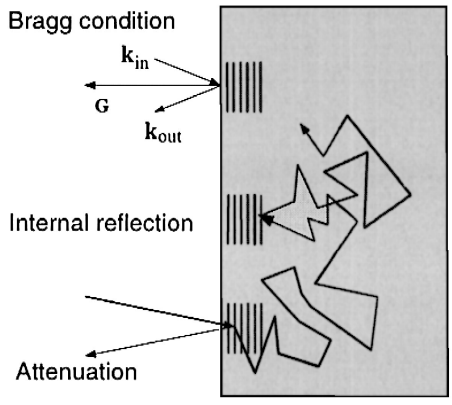

Fig. 3. The backscatter cone is affected by two mechanisms if the frequency is in a stop band. The cone is widened if the incident beam (lower left, bold arrow) is attenuated by Bragg scattering, i.e. if it matches the Bragg condition $\mathbf{k}_{out} - \mathbf{k}_{in} = \mathbf{G}$ for the [111] reciprocal lattice vector **G** (upper left corner). Light paths in the medium are internally reflected if they arrive at the sample boundary at an orientation matching the Bragg condition. The internal reflections create longer light paths, hence the cone is narrowed.

Extending the theory in Ref. [19] we find a broadening of the cone by a factor

$$\frac{\ell}{\ell_W} = \eta = \frac{(1+\tau_0)^2}{1+2\tau_0}\,\frac{\xi\left[1+2(\epsilon+\tau_e)\,\xi\right]}{\left[1+(\epsilon+\tau_e)\,\xi\right]^2} \qquad (1)$$

given a diffuse reflection coefficient R, and an attenuation length L_{att}^2. We have introduced the parameters ξ and ϵ according to

$$\xi = 1 + \frac{l}{L_{att}},\ \epsilon = \frac{R}{1-R} \qquad (2)$$

as well as the extrapolation length ratios $\tau_0 = z_0/\ell$ and $\tau_e = z_e/\ell$. The extrapolation length

$$z_e = z_0\frac{(1+R)}{(1-R)}$$

depends on the internal reflection coefficient. We take the extrapolation length z_0 equal to $z_0 = \frac{2}{3}\ell$ [19,21].

Since the L-gaps in the opals and air-sphere crystal extend over a cone of half apex angle $\gtrsim 0.2$ rad

[2] The factor η reduces to the familiar internal reflection [19] in the limit of a conventional random medium $L_{att} \to \infty$, i.e. $\xi \to 1$.

which is much larger than the typical width of the enhanced backscatter cones $\lesssim 20$ mrad, we have assumed an angle independent attenuation length. This assumption does not hold at frequencies close to the stop band edges. Analysis of η reveals that a broadening only occurs if the attenuation length is significantly shorter than the transport mean free path. A two-band model [22,23] predicts that the attenuation length $L_{\mathrm{att}} \approx 2.5\,\mu\mathrm{m}$ at the center of the L-gap. However, experimental studies indicate that the attenuation length is at least a factor two [24] to five [14,25] longer than predicted by theories which do predict the correct stop band frequencies and widths, such as the two-band model. The disagreement has been attributed to disorder in general [25] and planar stacking faults specifically [24]. If the magnitude of the attenuation length is a factor of five larger than predicted by the two-band model, it is of the order or the transport mean free path itself, so the effect of attenuation on the cone width is insignificant, i.e. $\xi \approx 1$. Apparently, it remains a challenge to interpret attenuation lenghts in photonic gaps, especially in the limit of high refractive index.

Relevant parameters such as the stop band width and the maximum solid angle of excluded directions are conveniently expressed in terms of the photonic strength parameter $\Psi = 4\pi(\alpha/v)g(Gr)$ where G is the length of the (111) reciprocal lattice vector, r is the sphere radius and $g(x) = 3(\sin x - x\cos x)/x^3$. Essentially the photonic strength parameter is the polarizability α per volume v [26], and it equals the relative width of the L-gap [27]. The maximum angular extent of the stop band is a cone of half apex angle approximately $\theta_{\max} = \arctan(\sqrt{2\Psi}) \approx \sqrt{2\Psi}$ [28]. We estimate the diffuse reflection coefficient by employing the procedure described in Ref. [21], replacing the directional reflection coefficient $R(\theta)$ by 1 for directions within a stop band, and 0 outside. This model predicts the maximum value $R \approx 4\Psi$ for the diffuse reflection coefficient, which would imply a narrowing of the cone by a factor ~ 1.4 for opals and ~ 2 for the air-sphere crystal[3]. The calculated diffuse reflection coefficient increases linearly with frequency from zero at the red edge to its maximum value at the blue edge, and decreases beyond the stop band, as the solid angle of excluded propagation directions diminishes. The effect of internal reflections due to the effective refractive index mismatch of the samples is negligible. Due to the complexity of the second and higher order Brillouin zones, we have not yet attempted to extend the model to the frequency range of higher order stop bands.

Apart from affecting the cone width, the cone shape is not significantly altered by the attenuation and reflection correction. The attenuation of the coherent beam can increase the contribution of single scattering, because the probability of a first scattering event far from the sample surface is decreased. In the polarization conserving channel, increased single scattering results in a reduction of the enhancement factor, which would appear for wavelengths within the stop band. Currently, more work must be done to understand the enhancement factors, especially for the air-sphere crystals.

5. Discussion

The solid curve in Fig. 2(a) results from the model presented in the previous section. The photonic strength parameter $\Psi = 0.07$ applicable to the opals (see Footnote 3) was used to calculate the diffuse reflection coefficient. We expect the cone to be unaffected by the photonic band structure for frequencies below the stop gap, for which a Bragg condition is never met. Consequently we scale the solid curve in Fig. 2(a), i.e. $\eta^{-1} = \ell_W/\ell$ as defined in Eq. (1), to match ℓ_W at the red edge of the stopband where $\ell_W = \ell$. The model contains no other adjustable parameter. As the wavelength is tuned into the stop band the theory predicts an increase of ℓ_W at the blue edge of the stop band which is due to the internal reflections. The predicted ratio between ℓ_W at the red side and ℓ_W at the blue side of the gap depends only on the internal reflection correction. At the blue edge the calculated diffuse reflection coefficient attains a maximum $R \approx 0.28$. The predicted increase by a factor $1/(1-R) \approx 1.4$ agrees with the data. For the more strongly photonic air-sphere crystals, the model (solid curve

[3] The values of Ψ were taken from the relative width $\Delta\omega/\omega_0$ of the L-gap stop bands, which are 0.07 for polystyrene opals and 0.13 for air-sphere crystals [15,16].

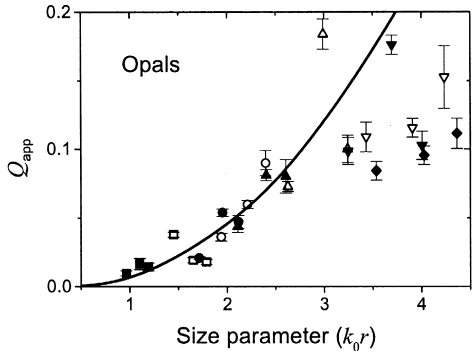

Fig. 4. The apparent scattering efficiency per sphere Q_{app} as a function of the size parameter, for radii 120 (■), 180 (□), 213 (●), 241 (○), 262 (▲), 326 (△), 403 (▼), 426 (▽), 439 nm (◆). The solid line is the Rayleigh–Gans scattering efficiency of a thin shell of refractive index 1 in an effective medium of refractive index 1.45 (see Footnote 4).

in Fig. 2(b)) also successfully explains the narrowing of the backscatter cones at the blue side of the stopgap relative to the red side by a factor ≈ 2 which is consistent with $R \approx 4\Psi \approx 0.5$ (see Footnote 3).

Finally we discuss a scattering mechanism which accounts for the order of magnitude of the transport mean free paths measured in the opals. As a simple model we propose that the scattering in the opals is mainly due to polydispersity of the spheres and small displacements from their lattice sites. The difference in refractive index profile of the displaced, slightly polydisperse Mie-spheres as compared to the ideal structure is a collection of thin shells of air and polystyrene. We have calculated the Rayleigh–Gans scattering efficiency [20] of spherical shells of refractive index 1[4] and radius r in an effective medium with index of refraction $n_e = 1.45$ for the opals. For comparison with the data we define the apparent scattering efficiency of each sphere in the opal as $Q_{app} = 1/(n\ell_W \pi r^2)$, where n is the sphere number density. As shown in Fig. 4, we observe that this simple shell model compares well to the data for shell thicknesses which are 5% of the nearest neighbor distance between spheres in the crystal. This value is consistent with the small sphere polydispersity of $\sim 2\%$, and with the estimated root mean square displacement u_{RMS}. In *fcc* crystals of polystyrene spheres in suspension at a volume fraction of 56% the displacement u_{RMS} was determined to be $\sim 3.5\%$ of the nearest neighbor distance [17]. In the more dense opals we estimate $u_{RMS} \lesssim 3.5\%$.

[4] The refractive index mismatch of air relative to the effective medium is much larger than the index mismatch of polystyrene. Consequently the scattering efficiency of polystyrene shells is only 10 % of the efficiency of air shells.

6. Conclusion

We have reported the first observations of enhanced backscattering of light by photonic crystals. The results indicate that the opals and the strongly photonic air-sphere crystals are weakly randomly scattering since the observed transport mean free paths are much longer than wavelengths in the visible. The transport mean free path also exceeds the typical periodicity length scale of the crystals, i.e. the (111) plane separation, by an order of magnitude. We have demonstrated that the cone shape is affected by the photonic band structure through two mechanisms. The inverse cone width is increased as a consequence of diffuse internal reflections which result from Bragg scattering, while it may decrease due to attenuation of the coherent beam which acts as a source of the diffuse intensity. An extension of the diffusion model incorporating these effects successfully explains the narrowing of the cones which is observed as the frequency is tuned from the red to the blue edge of the L-gap. The lack of reported experimental studies of the attenuation length hampers the accurate description of the increase in cone width in the stop band itself. We hope our work will stimulate further efforts to quantify the attenuation length in photonic crystals as a function of frequency and orientation.

Acknowledgements

The authors would like to acknowledge Henry van Driel for reflectivity measurements of the opals, and Judith Wijnhoven for sample preparation. We thank Frank Poelwijk, Frank Schuurmans and Henry Schriemer for help with experiments and valuable

discussions. This work is part of the research program of the ''Stichting voor Fundamenteel Onderzoek der Materie'', which is financially supported by the ''Nederlandse Organisatie voor Wetenschappelijk Onderzoek''.

References

[1] C.M. Soukoulis (Ed.), Photonic Band Gap Materials, Kluwer, Dordrecht, 1996.
[2] E. Yablonovitch, Phys. Rev. Lett. 58 (1987) 2059.
[3] S. John, Phys. Rev. Lett. 58 (1987) 2486.
[4] P.W. Anderson, Phys. Rev. 109 (1958) 1492.
[5] S. John, Phys. Rev. Lett. 53 (1984) 2169.
[6] D.S. Wiersma, P. Bartolini, A. Lagendijk, R. Righini, Nature 390 (1997) 671.
[7] F.J.P. Schuurmans, M. Megens, D. Vanmaekelbergh, A. Lagendijk, Phys. Rev. Lett. 83 (1999) 2183.
[8] Y. Kuga, A. Ishimaru, J. Opt. Soc. Am. A 8 (1984) 831.
[9] M.P. van Albada, A. Lagendijk, Phys. Rev. Lett. 55 (1985) 2692.
[10] P.E. Wolf, G. Maret, Phys. Rev. Lett. 55 (1985) 2696.
[11] E. Akkermans, P.E. Wolf, R. Maynard, Phys. Rev. Lett. 56 (1986) 1471.
[12] M.B. van der Mark, M.P. van Albada, A. Lagendijk, Phys. Rev. B 37 (1988) 3575.
[13] E.E. Gorodnichev, S.L. Dudarev, D.B. Rogozkin, M.I. Ryazanov, Sov. Phys. JETP 69 (1989) 1017.
[14] Yu.A. Vlasov, M.A. Kaliteevski, V.V. Nikolaev, Phys. Rev. B 60 (1999) 1555.
[15] J.E.G.J. Wijnhoven, W.L. Vos, Science 281 (1998) 802.
[16] M.S. Thijssen et al., Phys. Rev. Lett. 83 (1999) 2942.
[17] W.L. Vos, M. Megens, C.M. van Kats, P. Bösecke, Langmuir 13 (1997) 6004.
[18] D.S. Wiersma, M.P. van Albada, A. Lagendijk, Rev. Sci. Instrum. 66 (1995) 5473.
[19] A. Lagendijk, R. Vreeker, P. de Vries, Phys. Lett. A 136 (1989) 81.
[20] H.C. van der Hulst, Light Scattering by Small Particles, 1st ed., Dover, New York, 1981.
[21] J.X. Zhu, D.J. Pine, D.A. Weitz, Phys. Rev. A 44 (1991) 3948.
[22] K. Shung, Y. Tsai, Phys. Rev. B 48 (1993) 11265.
[23] R.J. Spry, D. Kosan, Appl. Spectrosc. 40 (1986) 782.
[24] J.F. Bertone et al., Phys. Rev. Lett. 83 (1999) 300.
[25] Yu.A. Vlasov, V.N. Astratov, O.Z. Karimov, A.A. Kaplyanskii, Phys. Rev. B 55 (1997) 13357.
[26] W.L. Vos et al., Phys. Rev. B 53 (1996) 16231.
[27] W.L. Vos, J.E.G.J. Wijnhoven, M. Megens, Conference on Lasers and Electro-Optics Europe, IEEE/LEOS, Piscataway, NJ, 1998, p. 361.
[28] M. Megens, J.E.G.J. Wijnhoven, A. Lagendijk, W.L. Vos, Phys. Rev. A 59 (1999) 4727.